



Photonic transfer through subwavelength optical waveguides

To cite this article: C. Girard *et al* 1998 *EPL* **44** 686

View the [article online](#) for updates and enhancements.

You may also like

- [Interstellar Objects from Broken Dyson Spheres](#)
Abraham Loeb
- [Dynamical equations for time-ordered Green's functions: from the Keldysh time-loop contour to equilibrium at finite and zero temperature](#)
H Ness and L K Dash
- [/IRAS-BASED WHOLE-SKY UPPER LIMIT ON DYSON SPHERES](#)
Richard A. Carrigan

Photonic transfer through subwavelength optical waveguides

C. GIRARD¹, A. DEREUX² and C. JOACHIM¹

¹ CEMES, UPR CNRS 8011 - 29 rue Jeanne Marvig, BP 4347
F-31055 Toulouse Cedex 4, France

² Laboratoire de Physique, Optique submicronique, ESA 5027 CNRS
Université de Bourgogne BP 400 - 21011 Dijon, France

(received 23 July 1998; accepted in final form 21 October 1998)

PACS. 02.90+p – Other topics in mathematical methods in physics.

PACS. 42.79–e – Optical elements, devices, and systems.

PACS. 42.70Qs – Photonic bandgap materials.

Abstract. – *Optical tunneling effect* through dielectric junctions with subwavelength transverse sizes has been demonstrated some years ago. In this letter, we demonstrate how similar effects can be exploited to perform photonic transfer through a *subwavelength optical waveguide* (SOW) by structuring its optical index along the direction of propagation. The optical transmittance of the SOW is computed self-consistently in direct space through the numerical solution of a Dyson equation. We apply this scheme to investigate the optical properties of different SOW architectures. Even under total internal reflection, in which the light is coupled to the SOW by an evanescent mode, an efficient optical transfer can be expected.

The common way of transferring optical energy between two dielectric media consists in connecting them with an optical waveguide. Traditionally such devices are fabricated with homogeneous materials and guide optical waves without losses over very large distances. According to the Rayleigh criterion [1], the smallest diameter of such optical waveguides is of the order of the incident wavelength λ . For transverse sizes smaller than λ , the incoming electromagnetic energy decays exponentially inside the guide along the direction of propagation (longitudinal direction).

Based on the Rayleigh criterion, most waveguides developed up to now appear to be homogeneous, *i.e.* without any optical index modulation along the longitudinal direction. However, breaking the homogeneity introduces new interesting properties. For example, introducing well-calibrated microcavities inside a channel waveguide modulates the optical transmittance of an initially homogeneous waveguide [2] and builds a photonic band structure in which some localized states can be created by adding localized defects in the linear periodic structure [3].

In a closely related context, the Rayleigh criterion is clearly broken by approaching a pointed fiber to detect the evanescent waves. In a sense, this is a way to detect the light by modulating the optical index as close as possible to the evanescent fields in order to convert them into

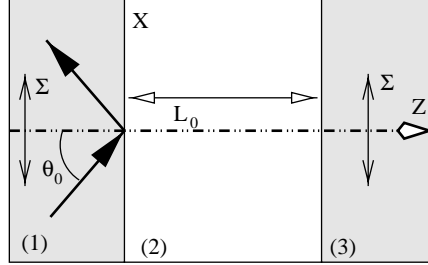


Fig. 1. – Schematic drawing of a planar optical junction composed by three dielectric media of optical index n_1 , n_2 and n_3 . L_0 represents the junction spacing. When the first medium is illuminated below the critical refraction angle the system is in the so-called *tunnel configuration*. Throughout all the paper this geometry will be considered as the reference system for the description of the excitation electromagnetic field $\{\mathbf{E}_0(\mathbf{r}, \omega), \mathbf{B}_0(\mathbf{r}, \omega)\}$ but also to define the initial field susceptibilities \mathbf{S}_0 and \mathbf{Q}_0 .

radiative waves [4-8]. The various results obtained in subwavelength optics raised several important questions concerning the physical mechanisms underlying photonic transport in mesoscopic and nanoscopic optical systems. For example, how is it possible to maintain the transmittance through an optical waveguide at a sufficiently useful level when its diameter is scaled down to a fraction of the incident wavelength? More precisely, what kind of relation between the guide diameter and the linear optical index modulation must be applied to enhance the photonic transfer efficiency? Very recently, an interesting gateway has been suggested in a work by Takahara *et al.* [9]. In this paper, a concept of nanometric tubular waveguide relies on the particular optical (plasmon) properties of a dielectric-metal interface of cylindrical shape. Although in real metal the efficiency of such guide designs is limited by the dielectric losses, they represent a first step toward the development of new nanometric optical-guide concepts.

In this paper, we analyze another fundamental mechanism to perform photonic transfer through a *subwavelength optical waveguide* (SOW) [10]. By structuring periodically the SOWs optical index along an appropriate direction, we demonstrate that even in the *subwavelength range* the opening of a *tunnel photonic band* allows a significant amount of energy to be transferred. The optical transmittance of the SOW is obtained numerically from a generalized propagator which is itself computed in direct space through a Dyson equation. We apply this scheme to investigate the optical properties of different SOW architectures. In particular, under total internal reflection illumination, in which the light is coupled to the SOW by an evanescent mode, it turns out that an efficient optical transfer can be expected.

In a first step, let us consider a simple optical junction formed by three dielectric media of optical indices n_1 , n_2 , and $n_3 = n_1$ (with $n_1 > n_2$, cf. fig. 1). When such a junction is illuminated in total internal reflection (TIR) from the first medium n_1 , its transmittance T (defined by the normalized energy flux transmitted in the third medium) displays a quasi-exponential decay with respect to the spacing L_0 [1]. Beyond the contact region, it can be approximated by

$$T(L_0) = A \exp[-\Gamma(\theta_0, k_0)L_0], \quad (1)$$

where, in this case, the decay factor $\Gamma = 2[n_1^2 \sin(\theta_0)^2 - n_2^2]k_0$ depends only on the incident angle θ_0 and the wave vector modulus k_0 in vacuum. The factor A depends on the polarization mode used to illuminate the system. According to this simple relation, beyond a certain spacing L_0 , equal to a few incident wavelengths, optical waves cannot reach the third medium anymore. This tunneling phenomenon is exploited in scanning near-field optical microscopy [4, 6, 8]

and also in nonresonant electron transfer through a tunnel barrier [11, 12]. Furthermore, by structuring the tunneling barrier either with an atomic [13] or a molecular wire [14], it was recently possible to understand and control the mechanisms governing this exponential decay in the tunneling regime [15]. On the other hand, the manifestation of electronic wave character leads also to the well-known quantification of the resistance in the ballistic regime [16] which is equivalent to the quantification of the transmittance in resonant optical energy transfer [17].

Now let us see what happens when a rod-shaped optical guide (optical index $n_{\text{ow}}(\mathbf{r})$) is connected between the incident (1) and the exit (3) media. In this case, both the initial evanescent electric and magnetic fields $\mathbf{E}_0(\mathbf{r}, \omega)$ and $\mathbf{B}_0(\mathbf{r}, \omega)$ are strongly modified by this rod. As demonstrated in ref. [18, 19] the new electromagnetic-field state $\{\mathcal{E}(\mathbf{r}, \omega), \mathcal{B}(\mathbf{r}, \omega)\}$ can be derived everywhere in the junction by introducing two generalized propagators labeled $\mathcal{K}(\mathbf{r}, \mathbf{r}', \omega)$ and $\mathcal{L}(\mathbf{r}, \mathbf{r}', \omega)$, respectively. If the SOW responds linearly to the excitation, the electric part $\mathcal{E}(\mathbf{r}, \omega)$ of the radiation can be described by the following linear relation:

$$\mathcal{E}(\mathbf{r}, \omega) = \int_v \mathcal{K}(\mathbf{r}, \mathbf{r}', \omega) \cdot \mathbf{E}_0(\mathbf{r}', \omega) d\mathbf{r}', \quad (2)$$

where the integral runs over the volume occupied by the optical wire. As detailed in ref. [18], the dyadic $\mathcal{K}(\mathbf{r}, \mathbf{r}', \omega)$, also called *generalized electric-field propagator*, can be formulated in terms of the optical-field susceptibility tensor $\mathcal{S}(\mathbf{r}, \mathbf{r}', \omega)$ associated with the entire system (SOW plus dielectric surrounding):

$$\mathcal{K}(\mathbf{r}, \mathbf{r}', \omega) = \delta(\mathbf{r} - \mathbf{r}') + \mathcal{S}(\mathbf{r}, \mathbf{r}', \omega) \cdot \chi_{\text{ow}}(\mathbf{r}', \omega), \quad (3)$$

where $\chi_{\text{ow}}(\mathbf{r}', \omega)$, the linear electric susceptibility of the optical waveguide, is merely related to its optical index by the relation

$$\chi_{\text{ow}}(\mathbf{r}', \omega) = \frac{(n_{\text{ow}}^2(\mathbf{r}', \omega) - 1)}{4\pi}. \quad (4)$$

The dyadic tensor $\mathcal{S}(\mathbf{r}, \mathbf{r}', \omega)$ in eq. (3) can be derived numerically by using Dyson's equation for the electric field

$$\begin{aligned} \mathcal{S}(\mathbf{r}, \mathbf{r}', \omega) &= \mathbf{S}_0(\mathbf{r}, \mathbf{r}', \omega) + \\ &+ \int_v \mathbf{S}_0(\mathbf{r}, \mathbf{r}', \omega) \cdot \chi_{\text{ow}}(\mathbf{r}', \omega) \cdot \mathcal{S}(\mathbf{r}, \mathbf{r}', \omega) d\mathbf{r}', \end{aligned} \quad (5)$$

in which $\mathbf{S}_0(\mathbf{r}, \mathbf{r}', \omega)$ is the field susceptibility associated with a homogeneous dielectric reference junction composed of two planar interfaces (cf. fig. 1). An analytical expression of this second-rank field susceptibility can be deduced from a pioneering paper by Agarwal [20]. In addition, other different numerical techniques available in the literature can be successfully applied to the calculation of such response function [21, 22].

In our electrodynamical treatment, the intrinsic optical properties of the SOW in interaction with its dielectric surroundings are completely contained in the dyadic $\mathcal{S}(\mathbf{r}, \mathbf{r}', \omega)$ which is the key ingredient to solve the problem. In the past, various matching boundary-conditions-based methods have been used for the calculation of $\mathcal{S}(\mathbf{r}, \mathbf{r}', \omega)$ near systems of simple symmetry (spheres, cylinders, planes, ...) [23]. With highly complex optical systems such as those considered here, other strategies must be adopted. As discussed in [18, 19], the recent developments of real-space approaches for electromagnetic scattering and light confinement established a powerful tool for the calculation of the electromagnetic response of optical systems composed of several domains of arbitrary shape and optical indices. In that scheme, the field susceptibility tensor \mathcal{S} required to obtain the *generalized field propagator* $\mathcal{K}(\mathbf{r}, \mathbf{r}', \omega)$, can be derived from

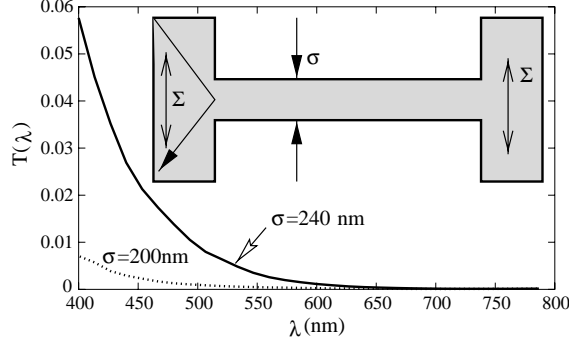


Fig. 2. – Variation of the transmittance of a subwavelength homogeneous optical wire (SOW) (cf. inset) as a function of the incident wavelength λ . In this simulation of the SOW transmission spectrum, the optical index n_{ow} is identical to the index of the bare optical junction ($n_{\text{ow}} = 1.5$) and $L_0 = 2.82 \mu\text{m}$. The calculation has been made in p -polarized mode and $\theta_0 = 46^\circ$.

the appropriate discretized form of a Dyson equation (5) over the whole volume occupied by the SOW:

$$\begin{aligned} \mathcal{S}(\mathbf{r}_i, \mathbf{r}_j, \omega) = & \mathbf{S}_0(\mathbf{r}_i, \mathbf{r}_j, \omega) + \\ & + \sum_{k=1}^n \chi_k(\mathbf{r}_k, \omega) \cdot \mathbf{S}_0(\mathbf{r}_i, \mathbf{r}_k, \omega) \cdot \mathcal{S}(\mathbf{r}_k, \mathbf{r}_j, \omega), \end{aligned} \quad (6)$$

where the entire SOW volume has been divided into n meshes of volume V_i centered at \mathbf{r}_i , ($i = 1 \dots n$), and

$$\chi_k(\mathbf{r}_i, \omega) = (n_{\text{ow}}^2(\mathbf{r}_i, \omega) - 1)V_i/4\pi \quad (7)$$

is directly related to the value taken by the optical index at a given position \mathbf{r}_i inside the optical waveguide. As an alternative to solving eq. (6) with a standard linear algebra procedure, we apply the iterative procedure described in [18], which allows to handle very large discretized systems accurately. From eq. (2), we can then compute both the electric and magnetic fields, $\mathcal{E}(\mathbf{r}, \omega)$ and $\mathcal{B}(\mathbf{r}, \omega)$, transmitted in the third medium (cf. fig. 1). The time-averaged Poynting vector field is then defined by

$$\mathcal{P}(\mathbf{r}) = \frac{1}{2} \Re\{\mathcal{E}(\mathbf{r}, \omega) \wedge \mathcal{B}^*(\mathbf{r}, \omega)\}. \quad (8)$$

Finally, from the information contained in eq. (8), we are able to define a transmission coefficient characterizing the optical transparency of the SOW. This quantity will be normalized with respect to the incident energy E_{inc} crossing a surface Σ located inside the input medium and centered around the SOW (cf. fig. 1 and inset of fig. 2):

$$T(L_0, \theta_0, \lambda) = \frac{\int_{\Sigma} \mathcal{P}(\mathbf{l}, L_0 + Z_{\Sigma}) \cdot \mathbf{u}_z d\mathbf{l}}{E_{\text{inc}}}, \quad (9)$$

where Z_{Σ} defined the location of the surface Σ in the *output* medium of the SOW, $\mathbf{l} = (x, y)$ and \mathbf{u}_z is a unit vector directed along the OZ-axis. In the following, we will apply this relation to perform a comparative analysis of two kinds of SOW, namely, homogeneous and periodically structured SOWs. In order to ensure a good convergence of the method, the mesh size used in the numerical works is $\Delta_x = \Delta_y = \Delta_z = 30 \text{ nm}$.

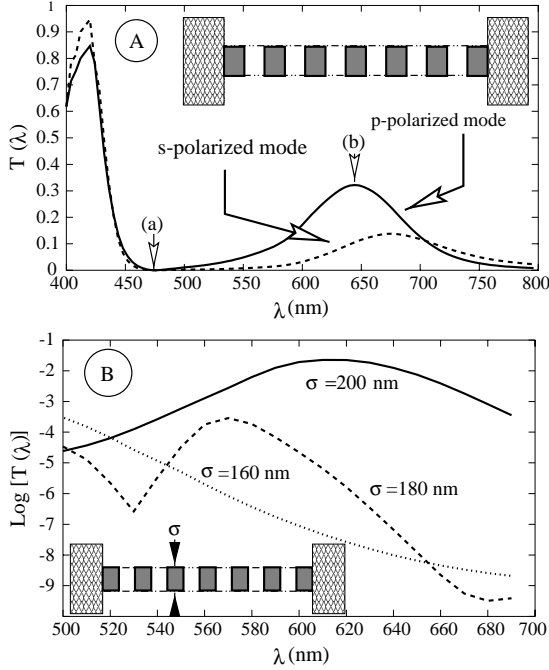


Fig. 3

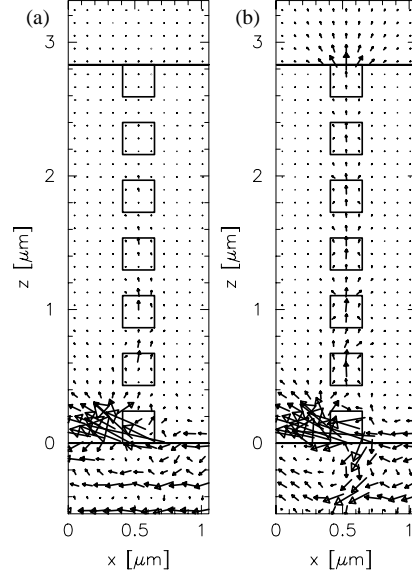


Fig. 4

Fig. 3. – (A) Same as fig. 2, but with a SOW structured with a periodic optical index modulation ($\sigma = 240$ nm). Around the solid curve (p -polarized mode) two working points (a) and (b) have been introduced to label regions of both weak and strong optical transparencies. (B) Evolution of the second tunnel photonic band as a function of the SOW diameter σ .

Fig. 4. – Planar projection of the time-averaged Poynting $\mathcal{P}(x, y = cst, z)$ vector in a (XOZ)-plane cutting the SOW center. (a) $\lambda = 475$ nm; (b) $\lambda = 640$ nm (see working points (a) and (b) defined in fig. 3A).

i) Homogeneous SOW (cf. fig. 2)

For this first application the function $n_{\text{ow}}(\mathbf{r})$ will be kept at the constant value 1.5 inside all the optical waveguide (this value is identical to the optical index of the two dielectric slabs connecting the SOW). For a typical SOW length $L_0 = 2.88 \mu\text{m}$, the two curves in fig. 2 clearly evidence the dramatic decay of the transmission coefficient *vs.* the incident wavelength when $\sigma < \lambda$. For example, around 640 nm and with a guide diameter constricted to 240 nm (dashed curve), the coefficient $T(L_0, \theta_0, \lambda)$ falls down to 10^{-3} . Although, optical guides with similar cross-sections can sustain propagation modes with real k -wave vectors (located around $\lambda = 400$ nm), they are not significantly excited when the guide is coupled by total internal reflection. Actually, the precise location of these modes would require an accurate calculation of the local density of photonic states.

ii) Periodically structured SOW (cf. figs. 3 and 4)

One of the main advantage of the formalism presented above lies in the fact that it can handle complex inhomogeneous systems formed by N distinct subdomains. Consequently, in our second application, we will use this opportunity to analyse similar transfer phenomena with SOWs of similar cross-section but composed by an alternance of two different materials

of optical indices $n_{\text{ow}}^{(1)}$ and $n_{\text{ow}}^{(2)}$ (see inset of fig. 3). In the present paper, all the numerical applications have been performed with a pattern period of 440 nm and two optical indices $n_{\text{ow}}^{(1)} = 1.0$ (air) and $n_{\text{ow}}^{(2)} = 2.2$ (dielectric). Differently from the dramatic decay of the transmission coefficient observed at the exit of homogeneous SOWs (fig. 2), the curves of fig. 3a (calculated for a cross-section $\sigma = 240$ nm) indicate a complete modification of the SOW spectrum. Although an exponential envelope still controls the transmission coefficient in the optical range, the opening of two tunnel photonic bands in the SOW enhance the photonic transfer efficiency around $\lambda_a = 425$ nm and $\lambda_b = 640$ nm, respectively. These two energy bands are generated by the localized states associated with the seven material structures that compose the SOW. They are broadened by the local surroundings and separated by an energy gap centered around the wavelength $\lambda_{\text{gap}} = 475$ nm. To complete this information, fig. 4 displays a map of the energy flow passing through the device for two typical wavelength values. In (a), when the *working point* is chosen in the gap, no significant energy transfer can be expected (see label (a) in fig. 3A). In (b), the efficiency increases drastically if the *working point* is translated towards the center of the second photonic band (see label (b) in fig. 3A).

In the visible range, these tunnel photonic bands considerably enhance the transfer process even for SOW with smaller transverse sizes (cf. fig. 3B). For example, the solid curve (calculated for $\sigma = 200$ nm) reveals an enhancement around the second peak of about three magnitude orders when passing from a homogeneous SOW (dashed curve of fig. 2) to an $n_{\text{ow}}^{(1)}$ periodically structured one. Finally, we note that for the optical-index variation considered in this application ($\Delta n = n_{\text{ow}}^{(2)} - n_{\text{ow}}^{(1)} = 1.2$), the extinction of the second peak only occurs for SOW diameters smaller than 160 nm (*i.e.* when $\sigma < \lambda/4$).

In conclusion, *optical tunneling effects* through *subwavelength optical waveguides* can be enhanced by an appropriate structuration of the guide index. Even under total internal reflection efficient transfer channels can be created. This effect can be exploited to perform usually forbidden photonic transfer between two arbitrary transparent media linked by a SOW. Independently of the fundamental interest of such a transfer mode involving high densities of evanescent waves, exploitation and optimization of such a concept could lead to the realization of interesting subwavelength optical devices that could be integrated in planar geometry.

One of us (AD) acknowledges the Council of Burgundy for financial support.

REFERENCES

- [1] BORN M. and WOLF E., *Principles of Optics* (Pergamon Press, Oxford) 1975.
- [2] VILLENEUVE P. R., FAN S., JOANNOPOULOS J. D., LIM K., CHEN J. C., PETRICH G. S., KOLODZIEJSKI L. A. and REIF R., in *Photonic Band Gap Materials, NATO ASI, Ser. E: Applied Sciences*, edited by C. M. SOUKOULIS, Vol. **315** (Kluwer, Dordrecht) 1996, pp. 411-426.
- [3] JOANNOPOULOS J. D., VILLENEUVE P. R. and FAN S., *Nature*, **386** (1997) 143.
- [4] REDDICK R. C., WARMACK R. J. and FERRELL T. L., *Phys. Rev. B*, **39** (1989) 767.
- [5] BETZIG E. and TRAUTMAN J. K., *Science*, **257** (1992) 189.
- [6] COURJON D. and BAINIER C., *Rep. Prog. Phys.*, **57** (1994) 989.
- [7] ZENHAUSEN F., MARTIN Y. and WICKRAMASINGHE H. K., *Science*, **269** (1995) 1083.
- [8] WEEBER J. C., BOURILLOT E., DEREUX A., GOUDONNET J. P., CHEN Y. and GIRARD C., *Phys. Rev. Lett.*, **77** (1996) 5332.
- [9] TAKAHARA J., YAMAGISHI S., TAKI H., MORIMOTO A. and KOBAYASHI T., *Optics Lett.*, **22** (1997) 475.
- [10] COURJON D., BAINIER C., GIRARD C. and VIGOUREUX J. M., *Ann. Phys. (Leipzig)*, **2** (1993) 149.

- [11] SIMMONS J. G., *J. Appl. Phys.*, **34** (1963) 1973.
- [12] BINNIG G. and ROHRER H., *Helv. Phys. Acta*, **55** (1982) 726.
- [13] YAZDANI A., EIGLER D. M. and LANG N. D., *Science*, **272** (1997) 1921.
- [14] VINUESA J. and JOACHIM C., *Europhys. Lett.*, **33** (1996) 635.
- [15] MAGOGA M. and JOACHIM C., *Phys. Rev. B*, **56** (1997) 4277.
- [16] VAN WEES B. J., VAN HOUTEN H., BEENAKKER C. W. J., WILLIAMSON J. G., KOUVENHIVEN L. P., VAN DER MAREL D. and FOXON C. T., *Phys. Rev. Lett.*, **60** (1988) 848.
- [17] MONTIE E. A., COSMAN E. C., HOOFT G. W., VAN DER MARK M. B. and BEENAKKER C. W. J., *Nature*, **350** (1991) 594.
- [18] MARTIN O. J. F., GIRARD C. and DEREUX A., *Phys. Rev. Lett.*, **74** (1995) 526.
- [19] GIRARD CH., WEEBER J. C., DEREUX A., MARTIN O. J. F. and GOUDONNET J. P., *Phys. Rev. B*, **55** (1997) 16487.
- [20] AGARWAL G. S., *Phys. Rev. A*, **11** (1975) 230.
- [21] GIRARD CH., MARTIN O. J. F. and DEREUX A., *Phys. Rev. Lett.*, **75** (1995) 3098.
- [22] GIRARD CH. and DEREUX A., *Rep. Prog. Phys.*, **59** (1996) 657.
- [23] METIU H., *Prog. Surf. Sci.*, **17** (1982) 153.